$Fr = u_0/[gd(\rho_0 - \rho_\infty)/\rho_0]^{1/2}$, densimetric Froude number
$H$ = enthalpy = $\lambda\omega + C_pT$
$r$ = radial coordinate
$\bar{r}_3$ = rate of formation of mass of liquid water per unit volume due to condensation
$T$ = temperature of vapor-air mixture
$T_d$ = droplet temperature
$u$ = axial velocity
$v$ = radial velocity
$z$ = axial coordinate

*Greek Symbols*

$\epsilon$ = eddy diffusivity of scalar (heat or water vapor)
$\lambda$ = heat of vaporization of water
$\rho$ = density of air + water vapor
$\theta$ = dimensionless passive scalar quantity
$\omega$ = mass fraction of water vapor in total gaseous species

*Subscripts*

$\infty$ = value in the ambient environment
cl = value at the jet center line
m = value along the mixing line (frozen jet case)
meas = a measured quantity
0 = value at nozzle effluent

*Superscripts*

$\bar{}$ = time smoothed quantity
* = corresponding to the value at local thermodynamic equilibrium or conditions at the surface of the droplet
$'$ = the turbulent fluctuation of a quantity
$\hat{}$ = dimensionless quantity

## Literature Cited


Bennett, D. Fog Formation and Vaporization in Turbulent Jets. M.S. Thesis, Carnegie Mellon University, 1971.
Chen, C. J.; Rodi, W. *Vertical Turbulent Buoyant Jets*; Pergamon Press: New York, 1980.
Hidy, G. M.; Friedlander, S. K. Vapor Condensation in the Mixing Zone of a Jet. *AIChE J.* **1964**, *1*, 115-123.
Hinze, J. O. *Turbulence*; McGraw-Hill: New York, 1975.
Matvejev, L. T. On the Formation and Development of Layer Clouds. *Tellus* **1964**, *16* (2), 139-146.
Schlichting, H. *Boundary-Layer Theory*; McGraw-Hill: New York, 1968.
Strum, M. L. Fog Formation in a Turbulent Jet. Ph.D. Thesis, Carnegie Mellon University, 1990.
Sunavala, P. D.; Hulse, C.; Thring, M. W. Mixing and Combustion in Free and Enclosed Turbulent Jet Diffusion Flames. *Combust. Flame* **1957**, *1*, 179-193.
Vatazhin, A. B.; Valeev, V. A.; Likhter, V. A.; Shulgin, V. I.; Yagodkin, V. I. Investigation of Turbulent Vapor-air Jets in the Presence of Condensation and the Injection of Foreign Particles. *Fluid Dyn.* **1984**, *3*, 385-392.
Vatazhin, A. B.; Valeev, V. A.; Likhter, V. A.; Shulgin, V. I. Turbulent Condensation Jets and the Possibilities of Their Control by Means of an Electric Field. *Fluid Mech.—Sov. Res.* **1985**, *14*, 10-22.


*Received for review* December 10, 1990
*Revised manuscript received* July 19, 1991
*Accepted* August 13, 1991

# History Effects in Transient Diffusion through Heterogeneous Media

**Joe D. Goddard**†
*Department of Chemical Engineering, University of Southern California, Los Angeles, California 90089-1211*

This article shows theoretically how scalar transport in a locally inhomogeneous medium characterized by variable capacity $c(\mathbf{x})$ and conductivity $\kappa(\mathbf{x})$ in the diffusion equation $c(\mathbf{x})\,\partial\psi/\partial t = \nabla\cdot\kappa(\mathbf{x})\nabla\psi + \gamma(\mathbf{x},t)$ can be represented by the homogenized form $\bar{c}*\partial\psi/\partial t = \bar{\kappa}*\nabla^2\psi + 1*\gamma$. Here $\bar{c}(t)$ and $\bar{\kappa}(t)$ are memory kernels and asterisks denote convolution integrals in $t$, which serve to represent the history effects arising from local diffusional relaxation. The analysis rests mainly on the effective medium approximation (EMA) applied to the lattice analogue or discretized version of the above equations. New EMA formulas are derived to account for the heterogeneous capacity $c(\mathbf{x})$ and the resulting history effect represented by $\bar{c}*\partial\psi/\partial t$. Also, based on symmetry arguments, new representations are given for the associated lattice Green's functions of general, non-Bravais lattices. In the short-time or high-frequency limit the discrete EMA predicts neither the diffusive response one expects of heterogeneous continua nor the wave-propagation effects that often accompany microscopic relaxation. Underlying reasons and the possible need for a nonlocal model involving higher order spatial gradients are discussed.

## 1. Introduction

**1.1. Transport Model.** We deal here with diffusive scalar transport in a locally isotropic heterogeneous medium which, with boldface symbols denoting physical vectors, is assumed to be governed by the well-known balance and flux relations

$$\frac{\partial\rho}{\partial t} + \nabla\cdot\mathbf{J} = \gamma \tag{1}$$

and

$$\mathbf{J} = -\kappa\nabla\psi \tag{2}$$

where, $\rho(\mathbf{x},t)$, $\mathbf{J}(\mathbf{x},t)$, and $\gamma(\mathbf{x},t)$ denote, respectively, a spatial density, associated vector flux, and volumetric source, while $\psi(\mathbf{x},t)$ is a potential and $\kappa = \kappa(\mathbf{x})$ a scalar conductivity. We assume continuity of $\psi$ at the interface between distinct phases, and we restrict ourselves to mathematically linear systems, on the basis of (2) and the further assumption

$$\rho = c\psi \tag{3}$$

where $c = c(\mathbf{x})$ is a volumetric capacity.

In any materially uniform region of space $\kappa$ and $c$ are constant, and (1)-(3) reduce to the diffusion equation:

$$\frac{\partial\psi}{\partial t} = D\nabla^2\psi + \frac{\gamma}{c} \tag{4}$$

where

$$D = \frac{\kappa}{c}\left[\frac{\text{area}}{\text{time}}\right] \tag{5}$$

† Present address: Department AMES-0310, University of California, San Diego, La Jolla, CA 92093-0310.

0888-5885/92/2631-0713$03.00/0 

is a diffusivity. The most familiar examples of (1)–(5) arise in the diffusion of heat or mass according to the classical laws of Fourier or Fick, respectively. In the former we identify $\psi$ as the temperature, $\kappa$ as thermal conductivity, $\mathbf{J}$ as heat flux, $\rho$ as energy density, and, hence, $c$ as volumetric heat capacity whereas, in the latter example, $\psi$ represents chemical potential, $\mathbf{J}$ mass flux, $\rho$ mass concentration, and $D$ molecular diffusivity, with the capacity $c$ representing in effect a chemical partition coefficient. Compressible Darcy flow in porous media provides yet another realization of (1)–(5).

In a microscopically heterogeneous medium $\kappa$ and $c$ vary spatially from point to point, as anticipated in (2) and (3). Provided this microscopic variation is sufficiently rapid compared to a relevant macroscopic length scale and has spatially independent mean, one expects that, for purposes of calculating scalar transport, any such medium can be represented by an effective homogeneous medium having locally uniform properties. Such "homogenization" (Ericksen et al., 1986; Sanchez-Palencia and Zaoui, 1987), and the determination of the corresponding constitutive equations, is a much studied question (Batchelor, 1974; Beran, 1968; Jeffrey, 1976; Hinch, 1977; Landauer, 1978), but most detailed treatments of scalar transport have been limited to the steady-state forms of (1)–(5) described by effective steady-state conductivities or diffusivities, $\kappa_\infty$ or $D_\infty$, say.

Although unsteady diffusion in heterogeneous media is often assumed to be governed by equations like (1)–(3), with $\kappa$ and $c$ replaced by $\kappa_\infty$ and $c_\infty$, this constitutes a *quasi-steady* approximation, valid only for sufficiently slow time variations of $\psi(\mathbf{x},t)$. For rapid variations we expect this approximation to fail, essentially because of capacitance effects and the associated diffusive relaxation process. Such failure could have important physical implications for the analysis of rapid transients or high-frequency diffusive response of materials and devices (Dogŭ et al., 1989; Phillips and Jansons, 1990). In the discrete electrical network analogue of (2) (Sahimi et al., 1983, Coniglio et al., 1989; Helsing and Grimvall, 1990) consisting of nodal junctions interconnected by resistors and connected to a common ground by individual capacitors, the neglect of capacitance is mathematically equivalent to a singular perturbation (Desoer and Shensa, 1970), which accounts for some of the inherent mathematical interest. We can formulate the quasi-steady approximation in terms of a nondimensional group:

$$\epsilon = \omega\tau \tag{6}$$

where $\omega$ is a characteristic frequency of excitation ($\partial/\partial t \sim \omega$) and $\tau$ is a microscopic relaxation time, defined in terms of a microstructural (correlation) length $l$ and a characteristic diffusivity $D^*$ by

$$\tau = l^2/D^* \tag{7}$$

This represents the characteristic time for establishment of microscale equilibrium (i.e., uniformity of $\psi$) by diffusion and plays a role analogous to the relaxation time in molecular systems. For $\epsilon \ll 1$ the transport coefficients are given by their low-frequency or long-time limits $\kappa_\infty$ and $c_\infty$ whose theoretical calculation represents a well-known problem for heterogeneous media. On the other hand, the high-frequency or short-time response for $\epsilon \to \infty$ is a much less well-studied problem and, to set the stage for the following analysis, we now consider a heuristic short-time diffusion model that is largely independent of microstructural detail.

In particular, we treat the well-known example of a statistically homogeneous isotropic two-phase system, with one phase having uniform properties $\kappa_2$, $c_2$, and volume fraction $\varphi$ embedded in a second phase of uniform properties $\kappa_1$, $c_1$, and volume fraction $1 - \varphi$. Consider then the transient response of a source-free medium to an abrupt discontinuity $[\psi] = 2$ imposed at time $t = 0$ on some smooth boundary or interior surface of a representative sample. From the classical treatments of (1)–(5), the normal component of surface flux into a region having uniform properties $c$ and $D$ is given by

$$J_n(t) = c(D/\pi t)^{1/2} \tag{8}$$

for small times $t > 0$ such that the characteristic penetration depth $(Dt)^{1/2}$ is small, in a sense to be specified more precisely below. In a heterogeneous medium any hypothetical surface cut will consist of exposed patches of the individual phases, presumably representative of the sample as a whole, hence, occupying respective areal fractions $\varphi$ and $1 - \varphi$. For extremely short times $t$ we expect these patches not to interact, so that we can simply sum up the independent normal flux contribution from each to obtain:

$$J_n(t) = (1 - \varphi)c_1\left(\frac{D_1}{\pi t}\right)^{1/2} + \varphi c_2\left(\frac{D_2}{\pi t}\right)^{1/2} \tag{9}$$

On identifying this with (8) for a hypothetical homogeneous medium having uniform properties $\kappa$, $D$, we obtain

$$cD^{1/2} = (1 - \varphi)c_1{D_1}^{1/2} + \varphi c_2{D_2}^{1/2} \tag{10}$$

Since this serves only to define the product $cD^{1/2}$, one needs a separate estimate of $c$, a question that will be considered further below. To be definite at this point, let us assume that the effective capacity should be identified with its equilibrium value:

$$c_\infty = (1 - \varphi)c_1 + \varphi c_2 \tag{11}$$

to yield from (10) the short-time (Goddard, 1985) estimate for diffusivity:

$$D_0 = \left[\frac{(1 - \varphi)c_1{D_1}^{1/2} + \varphi c_2{D_2}^{1/2}}{(1 - \varphi)c_1 + \varphi c_2}\right]^2 \tag{12}$$

In general, the condition of noninteracting phases and the estimate (12) can only be valid for times $t$ such that

$$t \ll \tau \tag{13}$$

where $\tau$ is a time constant of the form (7), with $l$ representing now the typical diameter or curvature radius of exposed surface patches.

An obvious generalization of (12) is

$${D_0}^{1/2} = \frac{\int_V c(\mathbf{x})D^{1/2}(\mathbf{x})\, dV\,(\mathbf{x})}{\int_V c(\mathbf{x})\, dV\,(\mathbf{x})} \tag{14}$$

for arbitrary distributions $c(\mathbf{x})$ and $D(\mathbf{x})$ over a macroscopic sample volume $V$. While later analysis will show that the estimate (11) and, hence, the denominator of (14) are not correct, it is nevertheless instructive to compare (14) to the one-dimensional theory of Gavalas and Yortsos (1980). They show, for short times near an initial discontinuity $[\psi] = 2$ at $x = 0$, that

$$\psi(x,t) \sim b^{1/4}\,\mathrm{erfc}\left\{\frac{x}{2[D_0(x)t]^{1/2}}\right\} \tag{15}$$

where

$$b = \frac{K(x)\,c(x)}{K(0)\,c(0)} \tag{16}$$

and where

$$D_0^{-1/2}(x) = \frac{1}{x}\int_0^x D^{-1/2}(x)\,dx \tag{17}$$

defines a spatial-average diffusivity $D_0(x)$ on $(0, x)$, an average somewhat different from that implied by (14) or (12). On the other hand, the flux at $x = 0$ is given by (15) to terms of leading order for $t \to 0$ as

$$J(0,t) = c(0)\left[\frac{D(0)}{\pi t}\right]^{1/2} \tag{18}$$

whose ensemble average gives a result identical with (14), provided that $c(\mathbf{x}) = c(0) =$ constant and that ensemble probabilities for $D(0)$ are identified in the usual way with spatial frequencies.

The discrepancy between (14) with $c(\mathbf{x}) =$ constant and (17) lies of course in the fact that (14) is valid on the time scales indicated by (13), whereas (17) becomes valid only after $t > O(\tau)$, such that the root-mean-square diffusive displacement $(Dt)^{1/2}$ is large enough to span a representative spatial distribution of $D(x)$. In either case, we can anticipate certain necessary restrictions on the spatial regularity of the $\kappa(\mathbf{x})$, $c(\mathbf{x})$ distributions, which in the case of two-phase systems and (12) amounts to a restriction on the regularity of the phase geometry. Thus, one can envisage geometries, such as fractal structures, that are so highly irregular as to violate the inequality (13) almost everywhere, no matter how small $t$ (Sahimi and Jerauld, 1983; Sahimi et al., 1983).

Whatever the microstructure, the notion of a time-dependent diffusivity or conductivity is most properly embodied in a continuum theory of *history-dependent* diffusion, in which the present flux $\mathbf{J}(\mathbf{x},t)$ depends on the entire past history of the potential gradient: $\nabla\psi(\mathbf{x},t')$, $-\infty < t' \le t$. While rarely stated, this idea is implicit in numerous discussion of transport in random media (e.g., in Ericksen et al. (1986), pp 107–119), which more often than not involve lattice or network models, sometimes envisaged as spatially discretized forms of (1)–(3) [e.g., Machta (1981), Sahimi et al. (1983), Silbey (1989)] as we shall do below. In the following we adopt, as a working hypothesis, a "simple-continuum" flux law involving only first-order spatial gradients, although we cannot definitively rule out more complex, nonlocal models involving longer range spatial effects. The latter would be manifested, for example, by the appearance of higher spatial gradients than those in relations like (2) or (19) below, or by more general integral relations (Luciani and Mora, 1983). A matter of long-standing concern in the mechanics of continuous media with microstructure [e.g., Green and Rivlin (1964), Mindlin (1964, 1965), Eringen et al. (1976)], such effects are also embodied in numerous models of wavelength-dependent transport pheomena, in "generalized" hydrodynamics [see Alder and Alley (1984)], in colloidal diffusion (Russel, 1981), and in dispersion in porous media (Koch and Brady, 1987). This matter will be taken up again below in the conclusions.

**1.2. History-Dependent Diffusion.** In a linear form appropiate to the present discussion, Gurtin and Pipkin (1968) have already proposed a continuum theory based on a generalization of "Cattaneo's law" of heat conduction, which is tantamount to the classical (Boltzmann) linear superposition and Stieltjes integral:

$$\mathbf{J}(\mathbf{x},t) = -\int_{-\infty}^{t}\kappa(t-t')\,d[\nabla\psi(\mathbf{x},t')] = -\int_0^{\infty}\kappa(\theta)\,d[\nabla\psi(\mathbf{x},t-\theta)] \tag{19}$$

where $\kappa(t)$ denotes a memory kernel or hereditary-influence function. Joseph and Preziosi (1989) have recently given an extensive review and treatment of the associated thermal wave propagation, in which much of the formalism is common to mechanical theories of viscoelasticity. For steady gradients $\nabla\psi$ one finds that (19) reduces to (2) with $\kappa = \kappa_\infty \equiv \kappa(\infty)$.

As will become apparent from the following analysis, we generally must also allow for a history-dependent capacity effect which, in place of (3), implies that

$$\rho(\mathbf{x},t) = \int_{-\infty}^{t} c(t-t')\,d\psi(\mathbf{x},t') \tag{20}$$

where $c(t)$ denotes an appropriate memory kernel, with $c = c_\infty = c(\infty)$ once again representing quasi-steady response. While one may argue abstractly for the breakdown of (3), owing to the influence of transport processes on what would normally be regarded as "thermodynamic" variables like $c$, a more compelling physical rationale emerges on considering the response to a spatially uniform, time-dependent source $\gamma(t)$ in a heterogeneous medium (such as a hypothetical uniform electric or dielectric heating of a heterogeneous thermal conductor) governed by (4) or (21) and (22) below. Even without external transport, one would in this situation expect the apparent overall capacitance to exhibit "time-lag" or history effects arising from internal diffusive relaxation.

For many initial-value problems and for the analysis to follow it is convenient to work in terms of Laplace transforms, in terms of which (1)–(5) become

$$L\hat{\psi}(\mathbf{x},s) = \sigma(\mathbf{x},s) \tag{21}$$

where circumflexes (ˆ) denote transforms, here and below, and where the linear operator $L$ is defined by

$$L[\,] = sc(\mathbf{x})[\,] - \nabla\cdot\kappa(\mathbf{x})\nabla[\,] \tag{22}$$

The transform variable $s$ is of course equivalent to the operator $\partial/\partial t$ and, hence, to $i\omega$ in the Fourier representation in $t$. The term $\sigma$ in (21) represents the combination of excitations due to an initial distribution $\psi(\mathbf{x},0)$ plus a source term $\hat{\gamma}(\mathbf{x},s)$. On the other hand, under the provisional assumption that homogenization leads to (19) and (20) in place of (2) and (3), we obtain the linear operator for our spatially uniform effective medium:

$$L_E[\,] = (1/s)\hat{L}_E[\,] = s\hat{c}(s)[\,] - \hat{\kappa}(s)\nabla^2[\,] \tag{23}$$

in the homogenized or "averaged-equation" (Hinch, 1977) version of (21), where $\hat{\kappa}(s)$ and $\hat{c}(s)$ are of transforms of the kernels $\kappa(t)$ and $c(t)$ in (19) and (20). Although we shall be concerned mainly with statistically isotropic media, some examples below involve anisotropic media. With only slight modification, most of the results would allow for anisotropy by means of a second-rank conductivity tensor $\hat{\kappa}(s)$ in (23).

## 2. Discrete Models and the EMA

We adopt the discrete or discretized versions of (21)–(23) already considered by numerous authors [see Sahimi et al. (1983), Coniglio et al. (1989), and Helsing and Grimvall (1990)], who discuss the analogies or applications to electrical resistor–capacitor (RC) networks:

$$\sum_j L_{ij}\hat{\psi}_j = \sigma_i \quad \text{or} \quad \underline{L}\,\underline{\hat{\psi}} = \underline{\sigma} \tag{24}$$

where underbars refer to $(N \times 1$ column) vectors and $(N \times N)$ matrices

$$\underline{\hat{\psi}} = [\hat{\psi}_i] \equiv [\hat{\psi}(\mathbf{x}_i,s)],\quad \underline{\sigma} = [\sigma_i] \equiv [\sigma(\mathbf{x}_i)] \tag{25}$$

and

$$\underline{L} = [L_{ij}] = [L(\mathbf{x}_i,\mathbf{x}_j,s)] \tag{26}$$

defined on network or lattice nodes $\mathbf{x}_i$ where $i, j = 1, 2, ..., N$ and the sum in (24) ranges in principle over all nodes. Here $L_{ij}$ has the form

$$L_{ij} = sC_i\delta_{ij} - A_{ij} \tag{27}$$

where

$$C_i = C(\mathbf{x}_i), \quad \delta_{ij} \equiv \delta(\mathbf{x}_i,\mathbf{x}_j) \tag{28}$$

and

$$A_{ij} = A_{ji} = A(\mathbf{x}_i,\mathbf{x}_j,s), \quad \text{with} \quad A_{ii} = -\sum_j A_{ij} \tag{29}$$

represent nodal capacity, nodal Kronecker delta, and bond conductance or admittance, respectively. In the electrical-network analogue, node $i$ is connected to node $j$ by resistance or admittance $A_{ij}$ and to common ground through capacitance $C_i$. The assumed symmetry of $\underline{A}$ corresponds to an elementary type of Onsager relation, a relation that would not apply to certain systems, such as diodes. At any rate, most of our results do not depend crucially on this assumption.

In the discretized form, the original randomly heterogeneous medium is represented in (27) by statistically capacitances $C_i$ and conductances $A_{ij} = K_{ij}$, independent of $s$. The problem of homogenization consists then of determining uniform capacitances $C_i = \bar{C} \equiv \hat{C}(s)$ and translation-invariant admittances

$$\bar{A}_{ij} \equiv \hat{K}_{ij}(s) \equiv \hat{K}(\mathbf{x}_i,\mathbf{x}_j,s) = \hat{K}(\mathbf{x}_i-\mathbf{x}_j,s) \tag{30}$$

which are ultimately to be associated with the operator in (23) and which define an effective operator $\underline{L}_E$ in (24). We note that, with the usual finite-difference or finite-element discretizations of continua, the capacitances and conductances (or admittances) are related to the original capacities and conductivities (or admittivities) by relations of the form $C = l^3c$ and $K = \kappa l$, where $l$ is a characteristic length comparable to that of (7).

The formal solution to the homogenization problem is given in terms of the Green's function or matrix $\underline{G} = \underline{L}^{-1}$ for (24)

$$\underline{G}_E = \langle \underline{G} \rangle \equiv \langle \underline{L}^{-1} \rangle \equiv \underline{L}_E^{-1} \tag{31}$$

where $\langle\ \rangle$ denotes a statistical average over $\underline{L}$, i.e., over $C_i$ and $L_{ij}$ (Elliot et al., 1974; Sahimi et al., 1983; Zaoui, 1987; Silbey, 1989). A similar formalism applies of course to the function-space operators (22) and (23), and our underlying assumption is that we may set up a physically reliable if not mathematically unique correspondence between discrete and continuum models.

Even in its simpler discretized form (30) the problem is virtually intractable by analytical means, as it involves determination of the averaged inverse of a large stochastic matrix. As a consequence, practically all existing analytical approaches rely on mathematical simplifications such as the well-known effective-medium or coherent-potential approximation ("EMA" or "CPA"), which we shall also employ here. Since the EMA and its applications to discrete systems have received much attention in the literature (Elliot et al., 1974; Landauer, 1978; Odagaki and Lax, 1981; Sahimi et al., 1983; Coniglio et al., 1989; Silbey, 1989), only the barest essentials are presented here, mainly to show the modification necessary for the case of variable capacities $C_i$ which does not seem to have been considered heretofore. Thus, decomposing $\underline{L}$ for the random medium into mean $\underline{L}_E$ and statistical fluctuation $\underline{L}'$ according to

$$\underline{L} = \underline{L}_E + \underline{L}' \tag{32}$$

one finds that the fluctuation in $\underline{G}$ is given, without approximation, by the matrix product

$$\underline{G}' \equiv \underline{G} - \underline{G}_E = -\underline{G}_E\underline{L}'(\underline{I} + \underline{G}_E\underline{L}')^{-1}\underline{G}_E \tag{33}$$

where $\underline{I} = [\delta_{ij}]$ is the idemfactor. The condition (31) requires that $\langle \underline{G}' \rangle$ vanish:

$$\langle \underline{L}'(\underline{I} + \underline{G}_E\underline{L}')^{-1} \rangle = \underline{0} \tag{34}$$

which is the EMA or CPA formula for $\underline{G}_E$ and, hence, $\underline{L}_E$ in terms of the statistical distribution of $\underline{L}'$.

We adopt the simplest EMA, in which the statistical fluctuation is attributed to only one node and an adjacent bond, say node $i = 1$ and its bond with $j = 2$, such that $C_1 \neq \bar{C}$ and $A_{12} = A_{21} \neq \bar{A}_{12} = \bar{A}_{21}$, whereas $C_i \equiv \bar{C}$ and $A_{ij} = \bar{A}_{ij}$ for all remaining nodes and bonds $i, j \neq 1, 2$, where $\bar{A}_{ij}$ are to be identified with the components $\hat{K}_{ij}(s)$ of $\underline{\hat{K}}(s)$ in the effective-medium operator

$$\underline{L}_E(s) = s\bar{C}\underline{I} - \underline{\hat{K}}(s) \tag{35}$$

Since all components of $\underline{L}'$ vanish, except $L'_{ij}$ for $i, j = 1, 2$, it follows by a slight but necessary extension of Odagaki and Lax (1981) that

$$\underline{L}'(\underline{I}' + \underline{G}_E\underline{L}')^{-1} = (1/\Delta)\{\underline{L}_0 + \underline{G}_0^{-1} \det \underline{G}_0 \det \underline{L}_0\} \tag{36}$$

where, with tr and det denoting trace and determinant,

$$\Delta = 1 + \text{tr}\,(\underline{G}_0\underline{L}_0) + \det \underline{G}_0 \det \underline{L}_0 \tag{37}$$

and

$$L_0 = \begin{bmatrix} L'_{11} & L'_{12} \\ L'_{21} & L'_{22} \end{bmatrix}, \quad \underline{G}_0 = \begin{bmatrix} \bar{G}_{11} & \bar{G}_{12} \\ \bar{G}_{21} & \bar{G}_{22} \end{bmatrix} \tag{38}$$

are $(2 \times 2)$ blocks extracted from the $(N \times N)$ matrices $\underline{L}'$ and $\underline{G}_E$, representing their restrictions to the range of $\underline{L}'$.

With the assumed Onsager symmetry, we have for the fluctuations that

$$-A'_{11} = A'_{12} = A'_{21} = -A'_{22} = a' \overset{\text{def}}{=} A_{12} - \bar{A}_{12} \quad \text{and} \quad c' \overset{\text{def}}{=} C_1 - \bar{C} \tag{39}$$

so that

$$L'_{11} = sc' - A'_{11} = sc' + a', \quad L'_{22} = -A'_{22} = a' \quad \text{and } L'_{12} = L'_{21} = -a' \tag{40}$$

whence, with $\bar{G}_{12} = \bar{G}_{21}$, we find by (36) and (37) that

$$\Delta = 1 + 2(\bar{G}_{11} - \bar{G}_{12})a' + s\bar{G}_{11}c' + (\bar{G}_{11}^2 - \bar{G}_{12}^2)sa'c' \tag{41}$$

and, as the basic EMA conditions, that

$$\left\langle \frac{c' + (\bar{G}_{11} - \bar{G}_{12})a'c'}{\Delta} \right\rangle = 0 \quad \text{and} \quad \left\langle \frac{a' + s\bar{G}_{12}a'c'}{\Delta} \right\rangle = 0 \tag{42}$$

where $a'$ and $c'$ are defined in (39) and the statistical averages $\langle\ \rangle$ are taken over $a'$ and $c'$, i.e., over a given joint-probability distribution of $C_1$ and $A_{12} \equiv K_{12}$.

In the case of uniform capacitance the fluctuation $c'$ vanishes identically, as does the first member of (42) while the second member reduces to the standard EMA result [Odagaki and Lax (1981) and subsequent works quoted immediately above]. Otherwise, and as an apparently new result, (42) involves simultaneous linear restrictions on $\langle a'/\Delta \rangle$, $\langle c'/\Delta \rangle$ and the cross-correlation $\langle a'c'/\Delta \rangle$, the latter of which can be associated with fluctuating capacitive–resistive interactions. In light of the analysis of Desoer and Shensa (1970) for electrical networks, one might expect

such effects to have profound consequences, especially for large $s$, i.e., short time. Given the joint statistical distribution of $C_1$ and $K_{12}$, (40)–(42) provide us with conditions on $\bar{C}$ and $\bar{K}_{12}$ and, hence, on the components, say $\bar{G}_{ij}$, of the effective medium Green's matrix $\underline{G}_E$. In order to employ (40)–(42), however, one must first express $\underline{G}_E$ in terms of $\hat{\underline{K}}$ through (31) and (35), which constitutes an important aspect of the EMA problem. As a slight digression, we now derive some generally useful formulas for the effective-medium Green's functions.

## 3. Lattice Green's Functions

Sahimi et al. (1983) and Silbey (1989) have given comprehensive reviews of existing techniques for deriving the Green's function in various Bravais and non-Bravais lattices, all of which involve simplifications depending in one way or another on the underlying network symmetries and the spatial range of nodal interactions. A generalization is presented here that allows one more easily to treat general lattices or periodic-cell models.

**3.1. Reductions Based on Lattice Symmetry.** While the translational invariance of such models makes them directly amenable to Fourier-transform algebra, it appears more direct and just as easy to employ the idea of a translation operator $\bigsqcup(\mathbf{r})$, such that

$$\bigsqcup(\mathbf{r})\, f(\mathbf{x}) = f(\mathbf{x}+\mathbf{r}) \tag{43}$$

for arbitrary functions of position $f(\mathbf{x})$ and, hence, such that

$$\bigsqcup(\mathbf{r}_2)\bigsqcup(\mathbf{r}_1) = \bigsqcup(\mathbf{r}_1)\bigsqcup(\mathbf{r}_2) = \bigsqcup(\mathbf{r}_1+\mathbf{r}_2) \quad \text{and} \quad \bigsqcup^{-1}(\mathbf{r}) = \bigsqcup(-\mathbf{r}) \tag{44}$$

Of course, for continuous fully differentiable functions of $\mathbf{x}$ the translation $\bigsqcup(\mathbf{r})$ corresponds to the differential operator $e^{\mathbf{r}\cdot\nabla}$, with the Fourier representation $e^{i\mathbf{k}\cdot\mathbf{r}}$ defining eigenvalues for the eigenfunctions $e^{i\mathbf{k}\cdot\mathbf{x}}$ for $\bigsqcup$. On the other hand, for discrete systems like (24), $\bigsqcup$ is defined only on arguments $\mathbf{r}_{ij} = \mathbf{x}_j - \mathbf{x}_i$, and $\bigsqcup(\mathbf{r}_{ij})$ can be envisaged as a supradiagonal matrix "shifter" transforming vector component $\psi_i = \psi(\mathbf{x}_i)$ into $\psi_j = \psi(\mathbf{x}_j)$. Except for Bravais lattices these translations do not represent primitive symmetry operations under which, by definition, all nodes are invariant. Rather, in any spatially periodic system in $d$ dimensions, charcterized by $d$ lattice vectors $\mathbf{l}_m$, $m = 1, 2, ..., d$, it is the set of elementary translations $\ell_m = \bigsqcup(\mathbf{l}_m)$, carrying unit cells into unit cells, which represent the primitive lattice symmetry.

To exploit the lattice symmetry, we employ an idea somewhat akin to renormalization (Burkhardt and van Leeuwen, 1982) by introducing a partition of the nodes $i = 1, 2, ..., N$ into unit cells, $I = 1, 2, ..., M$, with each cell containing $S = N/M$ distinct sites or nodes, and with each site having periodic replicates in all other cells, as illustrated in Figure 1. For brevity, let Greek indices $\alpha = 1, 2, ..., M^2$ refer to ordered pairs of cells $I, J$, with

$$\mathbf{r}_\alpha = \mathbf{r}_{IJ} = \mathbf{x}_J - \mathbf{x}_I \tag{45}$$

denoting separation between the pair, where $\mathbf{x}_I$ refers to some periodically replicated fiducial point or "origin" in each cell $I = 1, 2, ..., M$. The vector $\mathbf{r}_\alpha$ corresponds of course to a set of integers, say $\{\alpha_1, \alpha_2, ..., \alpha_d\}$, with $\alpha_i = 0, \pm1, \pm2, ...$, and with

$$\mathbf{r}_\alpha = \alpha_1\mathbf{l}_1 + \alpha_2\mathbf{l}_2 + ... + \alpha_d\mathbf{l}_d \tag{46}$$

representing the cell-to-cell translation

$$\ell^\alpha \overset{\text{def}}{=} \bigsqcup(\mathbf{r}_\alpha) = \ell_1^{\alpha_1}\ell_2^{\alpha_2}...\ell_d^{\alpha_d} \tag{47}$$

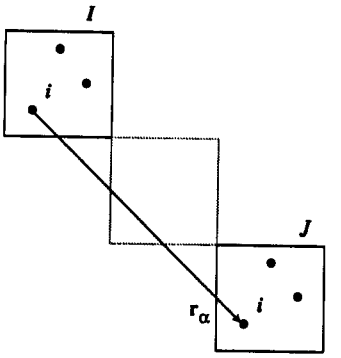


**Figure 1.** Two-dimensional schematic of a non-Bravais lattice with $S > 1$ distinct sites per unit cell.

for which, incidentally, the discrete Fourier transform is $\exp\{\alpha_1\mathbf{k}\cdot\mathbf{l}_1 + ... + \alpha_d\mathbf{k}\cdot\mathbf{l}_d\}$. The form (47) represents one element of the commutative (Abelian) translation symmetry group $\mathcal{T}$ for the lattice generated by the commutative basis $\ell_m$, $m = 1, 2, ..., d$. With the shorthand notation implied in (47) we can write

$$\ell^\alpha\ell^\beta = \ell^{\alpha+\beta} \tag{48}$$

where of course $\alpha + \beta$ refers to the set of exponents $\{\alpha_1 + \beta_1, ..., \alpha_d + \beta_d\}$ for $\ell_1, ..., \ell_d$.

The above partition of nodes into periodic cells is equivalent to the partition of vectors $\underline{\psi} = [\psi_i]$, $i = 1, 2, ..., N$, into blocks, corresponding to the direct sum:

$$\underline{\psi} = [\underline{\psi}_I] = \bigoplus_{I=1}^{M} \underline{\psi}_I \tag{49}$$

where $\underline{\psi}_I$ is a (column) vector of length $S$, representing the set of $S$ site potentials or probabilities for cell $I$. The above partition induces another partition and direct sum in the space of linear operators $\underline{L}$:

$$\underline{L} = [L_{ij}] = [\underline{L}_{IJ}] \equiv \bigoplus_{I,J=1}^{M} \underline{L}_{IJ} \tag{50}$$

where $\underline{L}_{IJ}$ is an $S \times S$ square matrix. Accordingly, equations of the form (24) read

$$\sum_{J=1}^{M} \underline{L}_{IJ}\underline{\psi}_J = \underline{\sigma}_I, \quad I = 1, 2, ..., M \tag{51}$$

Letting $\underline{L}$ refer now to the effective-medium operator $\underline{L}_E$, we have

$$\underline{L}_{IJ} = \bar{C}\delta_{IJ}\underline{\tilde{I}} - \underline{A}_{IJ} \tag{52}$$

where $\underline{\tilde{I}}$ denotes the $S \times S$ identity matrix, $\delta_{IJ} = \delta(\mathbf{x}_I,\mathbf{x}_J)$ the cellular Kronecker delta, and $\underline{A}_{IJ} \equiv \underline{\hat{K}}_{IJ}(s)$ an $S \times S$ matrix describing the coupling between cells. For $I \neq J$, $\underline{A}_{IJ}$ represents the admittance matrix for flow from $J$ to $I$, whereas for $I = J$ it describes intracellular exchange together with one-way transport from $I$ to all other cells.

We can make now further simplifications based on symmetry. First of all, given Onsager symmetry we expect that

$$\underline{A}_{IJ} = \underline{A}_{JI}^{\mathrm{T}} \tag{53}$$

Furthermore, because of the underlying invariance to the lattice symmetry group $\mathcal{T}$, we invoke the representation

$$\underline{A}_{IJ} = \underline{A}_\alpha\ell^\alpha \tag{54}$$

where $\ell^\alpha$ is defined in (47), and the $S \times S$ matrix $\underline{A}_\alpha = \underline{A}(\mathbf{r}_\alpha) \equiv \underline{A}(\alpha_1,...,\alpha_d)$ is equivalent to a Fourier component. In the present context $\underline{A}_\alpha$ represents the coupling between

pairs of cells $\alpha = (I, J)$ with $\alpha = 0$ referring to $I = J$ or $\alpha_1 = ... = \alpha_d = 0$. The range of the interaction between cells is now concisely expressed by the $\underline{A}_\alpha = \underline{A}(\mathbf{r}_\alpha)$ and, because of (53), one has that

$$\underline{A}_{-\alpha} = \underline{A}_\alpha^{\mathrm{T}} \tag{55}$$

where $-\alpha$ refers to $\{-\alpha_1, -\alpha_2, ..., -\alpha_d\}$. The standard model involving only nearest-neighbor interaction is thus represented by taking $\underline{A}_\alpha = \underline{0}$ for values of $\alpha_1, ..., \alpha_d$ other than $0, \pm 1$.

By means of (54) any equation of the form (51) can be expressed as

$$\tilde{\underline{L}}\underline{\psi}_I = \underline{\sigma}_I, \quad \forall I \tag{56}$$

where

$$\tilde{\underline{L}} = s\tilde{C}\tilde{\underline{I}} - \tilde{\underline{A}} \tag{57}$$

$$\tilde{\underline{A}} = \sum_\alpha \underline{A}_\alpha \ell^\alpha \tag{58}$$

involve only $S \times S$ matrices. The sum is understood to be taken over $\alpha_1, ..., \alpha_d = 0, \pm 1, \pm 2, ...$, and is subject to (53). Thus, lattice symmetry provides a reducible representation in which $\underline{L}$ is effectively diagonal, so that the problem of determining $\underline{G} = \underline{L}^{-1}$ (or any other analytic function of $\underline{L}$) is reduced to the vastly simpler one of determining an $S \times S$ matrix $\tilde{\underline{G}} = \tilde{\underline{L}}^{-1}$ (or the corresponding analytic function of $\tilde{\underline{L}}$). The $S \times S$ matrix $\tilde{\underline{G}}$ of course represents the diagonal blocks of $\underline{G}$ in the partition corresponding to (50).

**3.2. Representations for $\tilde{\underline{G}}$.** We shall occasionally make use in what follows of the integral representation

$$\underline{G} = \underline{L}^{-1} = \int_0^\infty e^{-q\underline{L}}\, dq \tag{59}$$

for essentially positive $\underline{L}$, i.e, for $\underline{L}$ with (eigenvalue) spectrum contained in the right half of the complex plane. This formula not only generates several known representations of lattice Green's functions but also makes it often easier to deduce the asymptotic behavior of $\underline{G}(s)$ for $s \to 0$ or $s \to \infty$. In the former limit, we recall that the condition of positive $\underline{L}$ is not satisfied for $d \leq 2$ leading to singularity of (59) (Sahimi et al., 1983).

Letting $\underline{A}$, $\underline{L}$, and $\underline{G}$ refer now to the matrices $\tilde{\underline{A}}$, $\tilde{\underline{L}}$, and $\tilde{\underline{G}}$, one immediately obtains a standard binomial expansion associated with (57):

$$\underline{L}^{-1} = \sum_{m=0}^{\infty} (s\tilde{C})^{-m-1}\underline{A}^m \tag{60}$$

by means of (59) and the exponential series for $e^{-q\underline{A}}$. Direct substitution of (58) into (60) leads to an expression of the form

$$\tilde{\underline{G}} = \sum_\alpha \underline{G}_\alpha \ell^\alpha \tag{61}$$

where the $S \times S$ matrices $\underline{G}_\alpha = \underline{G}_{IJ}$, representing the $S \times S$ matrix elements of the Green's matrix $\underline{G}$, are given as a complicated form in powers of the matrices $\underline{A}_\alpha$ in (58). In essence, $\underline{G}_\alpha$ represents the number of paths or statistical weight associated with lattice trajectory $\ell^\alpha$ defined by (47). Depending on circumstances, one or the other of the equivalent representations (59) and (60) may be more convenient. In either case, it is in principle possible to express $\underline{L}^{-1}$ as a matrix polynomial of maximum degree $S - 1$ in $\underline{A}$ by means of the HCS (Hamilton–Cayley–Silvester) theorems. We now consider some special cases where simplifications are possible.

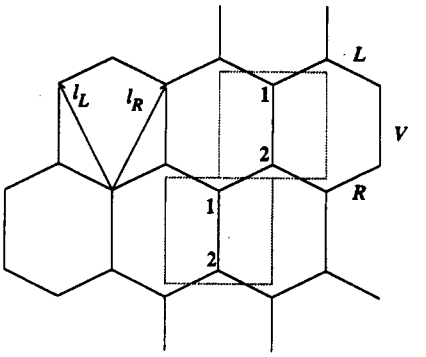


**Figure 2.** The two-dimensional honeycomb lattice, with (one possible choice of) unit cell and two distinct sites indicated.

With restriction to nearest-neighbor interactions between cells, the sum in (58) ranges over $\{\alpha_1, ..., \alpha_d\}$ such that $\alpha_m = 0, \pm 1$, for $m = 1, ..., d$, and can therefore be written

$$\tilde{\underline{A}} = \underline{B}_0 + \sum_{m=1}^{d} [\underline{B}_m \ell_m + \underline{B}_m^{\mathrm{T}} \ell_m^{-1}] \tag{62}$$

where we now have written $\underline{B}_m$, $m = 0, 1, 2, ..., d$ for the only possible distinct members of the set $\underline{A}_\alpha$. We now note a few instances for which the above formulas may be reduced further.

In the case of Bravais lattices, we may assign exactly one node to each unit cell, taking $S \equiv 1$ and $i, j, ... = I, J, ....$ The $\underline{B}_m$ in (62) simply become numbers $B_m$, say, representing nondirectional bond admittances along lattice directions $m = 1, 2, ..., d$, subject to

$$B_0 = -2\sum_{m=1}^{d} B_m \tag{63}$$

Making use of the generating function $\exp[\zeta(t+t^{-1})/2]$ for modified Bessel functions $I_n(\zeta)$ (Abramowitz and Stegun, (1965) eq 9.6.33), one obtains readily from (59):

$$\tilde{G}_\alpha = \int_0^\infty e^{-q(s\tilde{c}-B_0)} \prod_{m=1}^{d} I_{\alpha m}(2qB_m)\, dq \tag{64}$$

where $\alpha$ refers once again to $\{\alpha_1, \alpha_2, ..., \alpha_d\}$ with $\alpha_1, ..., \alpha_d = 0, \pm 1, \pm 2, ...$, $\tilde{G}_\alpha = G_\alpha \equiv G(\mathbf{r}_\alpha) \equiv G_{ij}$, and $\mathbf{r}_\alpha = \mathbf{x}_j - \mathbf{x}_i = \sum \alpha_m \mathbf{l}_m$. Since $B_m$ may have different values in different lattice directions, (64) represents an extension of previous results to anisotropic lattices, with the isotropic case, $B_m = B$, $m = 1, 2, ..., d$, representing cubic systems (Sahimi et al., 1983).

The above symmetry partition also allows for the treatment of certain non-Bravais lattices, illustrated by the two-dimensional "hexagonal" or honeycomb lattice in Figure 2. Here one may divide the lattice into square unit cells, with $S = 2$ distinct types of node per unit cell, and with bonds connecting alternate nodal types in different unit cells. One set of lattice vectors is represented by directed line segments $\ell_L$, $\ell_R$ connecting nodes of the same type situated in contiguous cells. There occur, therefore, three distinct $2 \times 2$ matrices $\underline{B}$ in (62), say

$$\underline{B}_0 = B_0\tilde{\underline{I}} + B_V(\underline{R} + \underline{R}^{\mathrm{T}}), \quad \underline{B}_1 \equiv \underline{B}_R = B_R\underline{R}, \quad \text{and} \quad \underline{B}_2 \equiv \underline{B}_L = B_L\underline{R}^{\mathrm{T}} \tag{65}$$

with

$$\underline{R} = \begin{bmatrix} 0 & 1 \\ 0 & 0 \end{bmatrix} \quad \text{and} \quad B_0 = -(B_R + B_L + B_V) \tag{66}$$

corresponding to $\ell_1 \equiv \ell_R = \coprod(\mathbf{l}_R)$, $\ell_2 \equiv \ell_L = \coprod(\mathbf{l}_L)$, where subscripts R, L, and V refer to the bond orientations (right-diagonal, left-diagonal, and vertical) in Figure 2. Thus, (57) and (62) yield

$$\underline{\tilde{L}} = (\bar{C}_s - B_0)\underline{\tilde{I}} - \underline{\Delta} \tag{67}$$

where

$$\Delta = \begin{bmatrix} 0 & \lambda \\ \lambda' & 0 \end{bmatrix} \tag{68}$$

with

$$\lambda = B_V + B_R\ell_R + B_L\ell_L \quad \text{and} \quad \lambda' = B_V + B_R\ell_R^{-1} + B_L\ell_L^{-1} \tag{69}$$

representing linear operators.

To obtain various forms for $\underline{\tilde{L}}^{-1}$, we note that

$$\underline{\Delta}^2 = \lambda\lambda'\underline{\tilde{I}} \tag{70}$$

and, hence, that any analytic matrix function $f(\underline{\Delta})$ is given by the odd–even decomposition

$$f(\underline{\Delta}) = \left[\frac{f(\lambda\lambda') + f(-\lambda\lambda')}{2}\right]\underline{\tilde{I}} + \left[\frac{f(\lambda\lambda') - f(-\lambda\lambda')}{2\lambda\lambda'}\right]\underline{\Delta} \tag{71}$$

by means of which one readily obtains from (67) that

$$\underline{\tilde{G}} = \underline{\tilde{L}}^{-1} = [(s\bar{C} - B_0)^2 - (\lambda\lambda')^2]^{-1}[(s\bar{C} - B_0)\underline{\tilde{I}} - \underline{\Delta}] \tag{72}$$

The problem is obviously reduced then to one of expressing the operator prefactor on the right-hand side of (72) in a convenient form. To this end, note that by (65)

$$\lambda\lambda' = B_V^2 + B_R^2 + B_L^2 + B_LB_R(\ell_H^{-1} + \ell_H) + B_RB_V(\ell_R + \ell_R^{-1}) + B_LB_V(\ell_L + \ell_L^{-1}) \tag{73}$$

where

$$\ell_H = \ell_R\ell_L^{-1} \tag{74}$$

represents a horizontal lattice translation in Figure 2. We also note that the translations appearing here can be expressed in terms of elementary translations $\mathcal{B}_V$, $\mathcal{B}_R$, $\mathcal{B}_L$ along bonds (V, R, L) in Figure 2 by $\ell_R = \mathcal{B}_R\mathcal{B}_V^{-1}$, $\ell_L = \mathcal{B}_L\mathcal{B}_V^{-1}$, and $\ell_H = \mathcal{B}_R\mathcal{B}_L^{-1}$. It is obvious that the binomial expansion of the prefactor in (72) would lead to a joint power series in $\ell_R$, $\ell_L$, in effect determining the various coefficients $\underline{G}_\alpha$ in (61). This is of course what would have been obtained directly from a binomial expansion of (67).

Alternatively, the $\underline{G}_\alpha$ can once again be expressed in terms of Bessel functions, by means of (67), (73), and (59). From these one obtains integrals involving $\exp\{[(s\bar{C} - B_0) \pm \lambda\lambda']q\}$, which on direct integration, lead back to (72), but which by (73) may instead be factored into a product of three generators for Bessel functions $\exp\{(\zeta/2)(\ell + \ell^{-1})\}$ involving the three translations $\ell$ in (72). Upon expansion one finally obtains $\underline{G}_\alpha = \underline{G}(\alpha_R,\alpha_L)$ in terms of an integral like (64), but now involving infinite sums of the form $\sum_n I_n(2qB_LB_R)I_{n-\alpha_R}(2qB_RB_V)I_{n-\alpha_L}(2qB_LB_V)$.

Finally, by interpreting the translations $\coprod(l)$ in (72) in terms of their Fourier transforms $e^{i\mathbf{k}\cdot\mathbf{l}}$, it appears that the Fourier inversion of (74) would lead to (elliptic) integral representation of the kind given in Sahimi et al. (1983). We shall not bother to make any of these results more explicit since the honeycomb lattice has served here merely to illustrate the above lattice-symmetry reductions. Rather, we return to the EMA and its consequences.

## 4. Short-Time Results and Conclusions

As amply clear from previous studies, the general complexity of the lattice Green's function $\underline{G}(s)$ precludes any detailed analytical treatment of EMA formulas such as (61). Thus, at best, one can extract asymptotic results for the long-time or short-time behavior of the memory kernels in (19) and (20), which asymptotes we recall correspond, respectively, to the limits $s \to 0$ and $s \to \infty$ in the transform domain. As the former limits has been treated extensively in previously works (Sahimi et al., 1983), we focus attention mainly on the latter, with the aim of assessing the EMA results against the heuristic result of the Introduction.

**4.1. Asymptotic EMA.** To illustrate the main ideas, we restrict attention at first to the one-dimensional case, where one may evaluate the integral in (64) exactly to give the components of $\underline{G}_E$ as

$$\bar{G}_{ij}(s) \equiv \bar{G}(n,s) = \frac{[h - (h^2 - 1)^{1/2}]^n}{2\bar{K}(h^2 - 1)^{1/2}} \tag{75}$$

where

$$n = |i - j|, \quad h = 1 + \frac{s\bar{\tau}}{2}, \quad \bar{\tau} = \frac{\bar{C}}{\bar{K}} \tag{76}$$

[cf. Sahimi et al. (1983)]. The quantity $\bar{\tau}$ represents an RC time parameter for the lattice. From (75) and (76) it follows that

$$\bar{G}_{12} \sim \bar{G}_{11} \sim \frac{1}{2}(\bar{K}\bar{C}s)^{-1/2} \quad \text{and} \quad \bar{G}_{11} - \bar{G}_{12} \sim \frac{1}{2\bar{K}}, \quad \text{for } s \to 0 \tag{77}$$

while

$$\bar{G}_{11} \sim \bar{G}_{11} - \bar{G}_{12} \sim \frac{1}{s\bar{C}} \quad \text{and} \quad \bar{G}_{12} \sim \frac{\bar{K}}{(s\bar{C})^2}, \quad \text{for } s \to \infty \tag{78}$$

where we have written $\bar{K}$ for $\bar{A} = \hat{A}_{12}(s)$. The EMA conditions (42) therefore become

$$\left\langle \frac{1}{K} - \frac{1}{\bar{K}} \right\rangle \to 0, \quad \text{and} \quad \left\langle (C - \bar{C})\left(\frac{1}{K} + \frac{1}{\bar{K}}\right)\right\rangle \to 0 \quad \text{for } s \to 0 \tag{79}$$

while

$$\left\langle \frac{1}{C} - \frac{1}{\bar{C}} \right\rangle \to 0, \quad \text{and} \quad \left\langle \frac{K}{C} - \frac{\bar{K}}{\bar{C}} \right\rangle \to 0 \quad \text{for } s \to \infty \tag{80}$$

Thus, in the long-time or quasi-steady limit the first relation in (79) gives a known result (Silbey, 1989) expressing the bond resistance $1/\bar{K}_\infty$ in the serial-resistance form $\langle 1/K \rangle$. While somewhat more complex, the second member of (79) shows that, to terms of order $\langle (C - \bar{C}_\infty)(K^{-1} - \bar{K}_\infty^{-1}) \rangle$, the capacitance $\bar{C}_\infty$ is given approximately by the parallel-capacitance form $\langle C \rangle$. By contrast, the short-time results (80) give the capacitance $\bar{C}_0$ as the serial capacitance $\langle C^{-1} \rangle^{-1}$ while the ratio $\bar{K}_0/\bar{C}_0$ representing diffusivity is given by the parallel-conduction form $\langle K/C \rangle$. That is, resistance and capacitance exhibit opposite modes of behavior, and the modes are reversed as one goes from short to long times.

On the basis of results like (64), the long-time behavior for spatial dimensions $d > 1$ has been treated in previous works (Sahimi et al., 1983) and will not be dealt with further here. On the other hand, for short times one sees immediately by (60) that there is no essential distinction for $s \to \infty$ between the cases $d = 1$ and $d > 1$, since such asymptotic forms apply irrespective of $d$. Therefore, one can generally expect the EMA in its present form to yield the serial-capacitor/parallel-resistor response (80) at short times, in any dimension $d$. While this result is at least partly in agreement with the result (10) of the Introduction, the exponent on diffusivity is quite different. In this respect, we encounter an understandable failure of the EMA to capture the continuum behavior reflected in (8), which is essentially a response to spatial excitations of large wavenumber and, hence, small wavelengths relative to the

microstructural length $l$ in (7).

Although it appears difficult to give a comprehensive analysis for disturbances of arbitrary wavelength, we can obtain a correspondence with (10) by simply replacing the previously assumed bond conductance $K = K_{12}$ by an admittance

$$A_{12} = K_{12}[1 + (sC_1/K_{12})^{1/2} + (sC_2/K_{12})^{1/2}] \quad (81)$$

The second and third terms in brackets, which represent response to a suddenly imposed potential difference across a single bond, derive basically from the formula (8) for one-dimensional transient conduction. In the guise of a parallel-conduction model (81) provides the most obvious interpolation between short-time and long-time asymptotes. For the short-time response, where the second and third terms in (81) dominate, we obtain by the second equation of (80)

$$\bar{A}/\bar{C} \sim \langle (sK_{12}C_1)^{1/2} + (sK_{12}C_2)^{1/2} \rangle \quad (82)$$

for $x \to \infty$. However, and consistent with discretization of our homogeneous effective continuum, we can also identify $\bar{A}$ with $\bar{K}$ and $\bar{C}$ through

$$\bar{A}/\bar{C} \sim 2(s\bar{K}\bar{C})^{1/2} \quad (83)$$

so that (82) and (83) yield

$$(\bar{K}\bar{C})^{1/2} \sim (1/2)[\langle (K_{12}C_1)^{1/2} \rangle + \langle (K_{12}C_2)^{1/2} \rangle] = \langle (KC)^{1/2} \rangle \quad (84)$$

for $x \to \infty$, the last equality following from statistical symmetry. Inspection shows this to be entirely equivalent to (9) for the two-phase medium. On the other hand, (11) provides an incorrect estimate of $\bar{c}$ and, with account now taken of the correct one:

$$c_0 = \langle c^{-1} \rangle^{-1} = [(1 - \varphi)c_1^{-1} + \varphi c_2^{-1}]^{-1} \quad (85)$$

the formula (14) must be replaced by

$$D_0^{1/2} = \frac{1}{V^2} \int_V c(\mathbf{x}) D^{1/2}(\mathbf{x})\, \mathrm{dV}(\mathbf{x}) \int_V c^{-1}(\mathbf{x})\, \mathrm{dV}(\mathbf{x}) \quad (86)$$

In addition to the above results for short times, one can also draw inferences about wave-propagation effects. In particular, in order that the differential operator (23) exhibit the wave-equation form $\partial^2/\partial t^2 - v^2\nabla^2$ in $\mathbf{x},t$ for short times $t$, the coefficients must satisfy $\hat{c}(s)/\hat{\kappa}(s) \sim s/v^2$ for $s \to \infty$, where $v$ represents a wave speed. In view of the discussion following (30), this implies that

$$\bar{\tau}(s) \sim (l^2/v^2)s \qquad \text{for } s \to \infty \quad (87)$$

where $\bar{\tau}$ is defined in (76) and $l$ is a microstructural length. However, according to the EMA result (80), $\bar{\tau}^{-1} \sim \langle K/C \rangle$, and in the models considered above $\langle K/C \rangle$ is given either as the average ratio of two quantities which are both independent of $s$ or else is given as an average $\langle A/C \rangle$ which exhibits $s^{1/2}$ diffusive response for $s \to \infty$. Therefore, we conclude that the above EMA models cannot, without further modifications, lead to real wave velocities and finite signal speeds which, in view of the underlying physical ideas and the RC-circuit analogue, is not surprising. As was the case for diffusive response, one must incorporate this feature into the underlying network model, for example, by inductive-type bond admittances or, more simply, by time lags representing finite transit delays. In other words, and in contrast to the overall history dependence revealed by the preceding analysis, no short-time rate effects emerge beyond those subsumed in the underlying discrete model.

**4.2. Conclusions.** The main findings are adequately summarized above in the abstract, where we have reverted to the time domain and a continuum description in $\mathbf{x}$. The convolution product appearing there is to be interpreted as the (unsymmetrical) bilinear form:

$$f*g(t) = \int_{-\infty}^{t} f(t-t')\, g(t')\, \mathrm{d}t' \quad (88)$$

on $(-\infty,t)$, which of course reduces to the standard (symmetrical) product for initial-value problems and functions defined on $(0,t)$.

As perhaps the major deficiency of the present work, no rigorous way has been found to derive the heuristic, quasi-continuum results (84)–(86) from the discrete EMA, a matter that relates to the question raised in the Introduction as to the necessity of nonlocal models in $\mathbf{x}$. In particular, one may envisage an effective continuum model like that of the abstract, in which $\bar{c}$ and $\bar{\kappa}$ are time-dependent differential operators $\bar{c}(t,\nabla)$, $\bar{\kappa}(t,\nabla)$, say, having Fourier–Laplace transforms $\hat{c}(s,\mathbf{k})$, $\hat{\kappa}(s,\mathbf{k})$ [cf. Koch and Brady (1987)]. In this case, formulas like (84)–(86) must be construed as arising from the combined high-frequency limits $s \to \infty$ and $|\mathbf{k}| \to \infty$. If so, then it is less than clear how time and space scales, which always occur in the present work in combinations such as (7), can be separated or how the same gradient effects for large $|\mathbf{k}|$ could emerge from a steady-state analysis for $s \to 0$. At any rate, the matter certainly deserves theoretical clarification.

## Acknowledgment

This work was supported in part by Grants NSF-CTS 8615160 and AFOSR 87-0284. History effects have not diminished the sentiments toward Professor Stuart Churchill expressed some 10 years ago in (the Acknowledgment) *Chem. Eng. Commun.* **1981**, *9*, 345. I trust he will see the formalism of the paper offered above as the wrapping and not the gift.

## Literature Cited

Abramowitz, M., Stegun, I. A. Eds. *Handbook of Mathematical Functions*; U.S. National Bureau of Standards: Washington, DC, 1965.

Alder, B. J.; Alley, W. E. Generalized Hydrodynamics. *Phys. Today* **1984**, *37*, 56–63.

Batchelor, G. K. Transport Properties of Two-Phase Materials with Random Microstructure. *Annu. Rev. Fluid Mech.* **1974**, *6*, 227–255.

Beran, M. *Statistical Continuum Theories*; Wiley: New York, 1968.

Burkhardt, T. W., van Leeuwen, J. M. J., Eds. Real Space Renormalization. *Top. Curr. Phys.* **1982**, *30*.

Coniglio, A.; Daoud, M.; Hermanns, H. J. Conductivity and Diffusion near the Percolation Threshold. *J. Phys. A: Math. Gen.* **1989**, *22*, 4189–4199.

Desoer, C. A.; Shensa, M. J. Networks with Very Small and Very Large Parasitics: Natural Frequencies and Stability. *Proc. IEEE* **1970**, *58*, 1933–1938.

Doğu, G.; Mürtezaoğlu, K.; Doğu, T. A Dynamic Method for the Effective Thermal Conductivity of Porous Solids. *AIChE J.* **1989**, *35*, 683–689.

Elliot, R. J.; Krumhansl, J. A.; Leath, P. L. The Theory and Properties of Randomly Disordered Crystals and Related Physical Systems. *Rev. Mod. Phys.* **1974**, *46*, 465–543.

Erdêyi, A. et al., Eds. *Higher Transcendental Functions*; McGraw-Hill: New York, 1953; Vol. 2, p 91 ff.

Ericksen, J. L.; Kinderlehrer, D.; Kohn, R.; Lions, J.-L., Eds. *Homogenization and Effective Moduli of Materials and Media*; Springer-Verlag: Berlin, 1986.

Eringen, C. A., Ed. *Continuum Physics*; Academic Press: New York, 1976; Vol. 4.

Gavalas, G. R.; Yortsos, Y. C. Short-Time Asymptotic Solutions of the Heat Conduction Equation and Spatially Varying Coefficients. *J. Inst. Math. Applic.* **1980**, *26*, 209–219.

Goddard, J. D. Memory Effects with Transient Diffusion in Heterogeneous Media. Presented at the Annual AIChE Meeting, Chicago, IL, 1985; Paper 13h.

Green, A. E.; Rivlin, R. S. Simple Force and Stress Multipoles. *Arch. Ration. Mech. Anal.* **1964**, *16*, 325-353.
Gurtin, M. E.; Pipkin, A. C. A General Theory of Heat Conduction with Finite Wave Speeds. *Arch. Ration. Mech. Anal.* **1968**, *31*, 113.
Helsing, J.; Grimvall, G. R. Conductance in Random Inductance-Capacitor Networks. *Phys. Rev B* **1990**, *31*, 113-126.
Hinch, E. J. An Averaged-Equation Approch to Particle Interactions in a Fluid Suspension. *J. Fluid Mech.* **1977**, *83*, 695-720.
Jeffrey, D. J. On the Averaged-Equation Approach to Conduction through a Suspension. *Arch. Mech.* **1976**, *28*, 423-429.
Joseph, D. D.; Preziosi, L. Heat Waves. *Rev. Mod. Phys.* **1989**, *61*, 41-73; Addendum **1990**, *62*, 375-391.
Koch, D. L.; Brady, J. F. Nonlocal Dispersion in Porous Media: Nonmechanical Effects. *Chem. Eng. Sci.* **1987**, *42*, 1377-1392.
Landauer, R. Electrical Conductivity in Inhomogeneous Media. In *Transport and Optical Properties of Inhomogeneous Media*; Garland, J. C., Tanner, D. B., Eds.; AIP Conference Proceedings 40; American Institute of Physics: New York, 1978.
Luciani, J. F.; Mora, P. Nonlocal Heat Transport Due to Steep Temperature Gradients. *Phys. Rev. Lett.* **1983**, *51*, 1664-1667.
Machta, J. Generalized Diffusion Coefficient in One Dimensional Random Walks with Static Disorder. *Phys. Rev. B* **1981**, *24*, 5260-5269.
Mindlin, R. D. Microstructure in Linear Elasticity. *Arch. Ration. Mech. Anal.* **1964**, *16*, 51-78.
Mindlin, R. D. Second Gradient of Strain and Surface Tension in Linear Elasticity. *Int. J. Solids Struct.* **1965**, *1*, 417-438.
Odagaki, T.; Lax, M. Coherent-Medium Approximations in the Stochastic Transport Theory of Random Media. *Phys. Rev. B* **1981**, *24*, 5284-5294.
Papanicolaou, G., Ed. *Random Media*; Springer-Verlag: Berlin, 1987.
Phillips, C. G.; Jansons, K. M. The Short-Time Transient of Diffusion outside a Conducting Body. *Proc. R. Soc. London, A* **1990**, *428*, 431-449.
Russel, W. B. Brownian Motion of Small Particles Suspended in Liquids. *Annu. Rev. Fluid Mech.* **1981**, *13*, 425-455.
Sahimi, M.; Jerauld, G. R. Random Walks on Percolation Clusters at the Percolation Threshold. *J. Phys. C: Solid State Phys.* **1983**, *16*, L1043-L1050.
Sahimi, M.; Hughes, B. D.; Scriven, L.; Davis, H. T. Stochastic Transport in Disordered Systems. *J. Chem. Phys.* **1983**, *73*, 6849-6864.
Sanchez-Palencia, E., Zaoui, A., Eds. *Homogenization Techniques for Composite Media*; Springer-Verlag; Berlin, 1987.
Silbey, R. Dynamical Processes in Disordered Systems. In *Disordered Solids. Structures and Processes*; DiBartolo, B.; Ożen, G., Collins, J. M., Eds.; Plenum Press: New York, 1989; pp 31-54.
Zaoui, A. In *Homogenization Techniques for Composite Media*, Sanchez-Palencia, E., Zaoui, A., Eds.; Springer-Verlag: Berlin, 1987; part VI.

*Received for review* November 26, 1990
*Revised manuscript received* March 21, 1991
*Accepted* April 19, 1991

# Mechanisms for Ion and Water Transport across Tracheal Epithelium

**Irving F. Miller**

*Department of Chemical Engineering (M/C 110), University of Illinois at Chicago, Chicago, Illinois 60680*

To explain the mechanisms whereby ions and water transport across trachael epithelium, we have developed a new hypothesis in which the principal event is $Na^+$-driven paracellular electroosmotic transport through dynamically controlled tight junctions. Upon stimulation, epithelial cell apical membrane impedance is reduced, resulting in net $Cl^-$ ion and water flux out of the cells, opening the cation-selective tight junctions, perhaps by activating apical perijunctional actomyosin rings. $Na^+$ flows through the tight junctions from serosa to lumen, in response to an electrochemical gradient developed by transcellular $Cl^-$ transport from serosa to lumen, pumping water electroosmotically. The $Na^+$ returns to the serosal side transcellularly, thus completing the circuit. Thus, water transport is directly coupled to $Cl^-$ transport, and impaired $Cl^-$ transport, as occurs for example in cystic fibrosis, directly results in impaired water transport.

## Introduction

Diseases of the airways of the lungs are among the major causes of morbidity and mortality in the United States, with approximately 17 million people suffering from chronic bronchitis, asthma, cystic fibrosis, or emphysema. These diseases are often caused or aggravated by such inhaled pollutants as cigarette smoke, sulfur dioxide, or allergens, thus underscoring the role of the lungs as the first line of defense of the body against the effects of inhaled particles, pollutants, and toxicants. Healthy lungs react to environmental challenges primarily by activation of the mucociliary clearance system, shown in the cross section of the epithelial tissue in Figure 1.

The respiratory tract ciliated epithelium is covered by a thin layer of fluid consisting of an aqueous periciliary layer bathing the cilia and a blanket, or islands, of viscoelastic mucus (Van As and Webster, 1974). Inhaled pollutants are trapped in the mucus layer, which is propelled by the beating cilia along the periciliary layer up the trachea and out of the lungs. The cilia beat in an asymmetric pattern, with an active stroke in the direction of the mouth, in which the tips of the cilia contact the mucus layer, and a return stroke in the distal direction, in which the cilia move through the periciliary layer without contacting the mucus. Adjacent cilia beat slightly out of phase, establishing sinusoidal metachronal waves that generally move mouthward up the trachea.

The mucociliary clearance system, consisting of the cilia, the mucus, and the periciliary layer, has both a basal and a stimulatory component. When the healthy system is at rest, the cilia beat at a base frequency that, in the dog, ranges over 6-12 Hz (Wong et al., 1986, 1988) and exert a force on the mucus layer estimated at $10^{-12}$ N/cilium (Yates et al., 1980). The periciliary layer is maintained at a thickness about 0.5 $\mu$m less than the length of a cilium (about 6 $\mu$m), and sufficient mucus is produced to provide a steady movement of the layer up the airways. When the system is stimulated, ciliary beat frequency (CBF), mucin release, and epithelial transport of water and ions all increase to provide an increased mucociliary transport.

The physical properties of the mucus and the efficiency of mucociliary clearance from the trachea are controlled by the interaction of several epithelial cell types, some of which perform ion and water transport, while others syn-

0888-5885/92/2631-0721$03.00/0 